Eur. Phys. J. B **60**, 305–312 (2007)
DOI: 10.1140/epjb/e2007-00350-9

THE EUROPEAN PHYSICAL JOURNAL B

Structural and optical properties of vanadium and hafnium nitride nanoscale films: effect of stoichiometry

H. Gueddaoui[1,2], S. Maabed[1], G. Schmerber[3], M. Guemmaz[1], and J.C. Parlebas[3,a]

[1] Laboratoire DAC, Faculté des Sciences, Université Ferhat Abbas, 19000 Sétif, Algeria
[2] USTHB, Faculté de Physique, Bab-Ezzouar, 16111 Alger, Algeria
[3] IPCMS, UMR 7504 CNRS-ULP, 23 rue du Loess, 67034 Strasbourg Cedex 2, France

Received 6 February 2006 / Received in final form 23 November 2007
Published online 22 December 2007 –

Abstract. Vanadium and hafnium nitride nanoscale films were synthesized onto (100)-oriented silicon wafers by reactive dc-magnetron sputtering. The temperature of the substrate was fixed at 150 °C. Several analysis techniques were used to characterize the resulting films: Wave Dispersion Spectroscopy (WDS) to determine nitrogen concentration, X-ray Diffraction (XRD) to study crystallographic structures, X-ray Reflectivity (XRR) to estimate their thicknesses and finally optical spectrophotometry (UV-Vis-IR) to measure the optical reflectance. The experimental conditions were selected in order to achieve two goals. The first one is to obtain ultra thin films (in the nanoscale range). The second one is to compare two symmetric systems, in terms of stoichiometry: over-stoichiometric hafnium nitrides and sub-stoichiometric vanadium nitrides. The XRR results showed that all synthesized films approximately presented the same thickness in the nanoscale range (less than 70 nm). The nitrogen concentration, measured by means of WDS, was in the sub-stoichiometric region for vanadium nitrides (N/V atomic ratio between 0.78 and 0.83) and over-stoichiometric region for hafnium nitrides (N/Hf atomic ratio between 1.18 and 1.25). From XRD patterns, the crystallographic film structure was found to be of NaCl type for the two systems, δ-VN and δ-HfN, with an amorphous part in the first system. Optical constants were derived from experimental reflectance spectra. Good agreement was found between experimental and calculated reflectance spectra using Drude and extended Drude models.

PACS. 68.55.-a Thin film structure and morphology – 81.15.Cd Deposition by sputtering – 78.66.-w Optical properties of specific thin films

1 Introduction

Transition metal nitrides have been the subject of intense studies, both theoretically and experimentally, due to their interesting properties (high melting point, chemical stability and corrosion resistance) [1–4], and references therein. Vanadium nitrides and hafnium nitrides systems are used in differing domains, especially in high technologies [5,6]. The main property of vanadium and hafnium nitrides and similar systems is the existence of defective structures with many deviations from stoichiometry. The physical and chemical properties of these systems are extremely sensitive to film microstructures and growth morphologies as well as deviations from stoichiometry. Non-stoichiometry is often a consequence of the presence of vacancies in the structure, either on metallic or nitrogen sites. VN systems have been much less studied than similar systems like TiN. In a previous paper [7] we showed that physical properties of VN films deposited by dc-magnetron sputtering strongly depend on deposition parameters, like nitrogen gas flow and substrate temperature. Similarly we studied the physical properties of sputtered HfN thin films [8].

In this work, we focused our attention on the evolution of optical properties versus stoichiometry. To carry out a good comparison, we chose to study two symmetrical systems, in terms of stoichiometry. The first one is sub-stoichiometric (vanadium nitride) and the second one is over-stoichiometric (hafnium nitride). Let us notice that electrical properties of HfN thin films have already been studied elsewhere [8]. In the present paper, by using a Drude model as well as an extended Drude model, we derived optical constants n (refraction index) and k

[a] e-mail: parlebas@ipcms.u-strasbg.fr

Table 1. Experimental synthesis conditions for HfN and VN films.

Sample	Gas flow (sccm) Nitrogen	Argon	Current (mA)	Substrate	Substrate temperature (°C)	Deposition time (s)	Thickness (nm)	Deposition rate (Å/s)
HfN4	4	20	800	Si(100)	150	80	50	6.25
HfN5	5					85	58.5	6.89
HfN6	6					90	53.6	5.96
HfN7	7					95	52.5	5.53

Sample	Gas flow (sccm) Nitrogen	Argon	Current (mA)	Substrate	Substrate temperature (°C)	Deposition time (s)	Thickness (nm)	Deposition rate (Å/s)
VN6	6	20	800	Si(100)	150	220	64.2	2.47
VN8	8					300	66.6	2.22
VN10	10					320	62.8	1.96
VN12	12					340	63.8	1.88

(extinction coefficient) of VN and HfN films. Let us just mention that several works were based on Kramers-Krönig integrations and ellipsometry in order to determine optical constants (n and k) of various films (see typically Refs. [9–11] and therein). Section 2 is devoted to the experimental procedure of preparation and characterization of the considered deposited samples, whereas in Section 3 we present and discuss our experimental results: structural and optical properties. We conclude by gathering the main results of this work.

2 Experimental procedure

VN and HfN films were deposited at 150 °C on n-type (100)-oriented silicon wafers by reactive dc-magnetron sputtering. Pure hafnium and vanadium discs (82.5 mm in diameter, 6 mm thick) were used as targets. Before deposition, Si(100) substrates were ultrasonically cleaned for 10 min, successively in acetone and ethanol, and then dried under a nitrogen gas flow. The vacuum chamber was evacuated by a rotary mechanical pump associated to a cryogenic pump. The argon and nitrogen gas flows were controlled by flowmeters. The pressure in the chamber was monitored by a Pirani–Penning gauge combination. Also before deposition, the sputtering chamber pressure was reduced to 2×10^{-8} mbar. Then a constant argon gas flow of 20 sccm was let into the chamber. The targets, as well as the substrates, were pre-sputtered during about 30 min in a pure argon atmosphere in order to remove carbon contamination and surface oxide layer (native oxide). The amount of nitrogen in the working gas was changed in the range from 0 to 7 sccm for HfN films and in the range from 0 to 12 sccm for VN films. The corresponding samples are labeled as VNn or HfNn where $n = 0; 1; 2; \ldots$ indicates the value of nitrogen flow expressed in sccm. The target to substrate distance was approximately 200 mm and the direct current discharge power was about 285 W. In this paper, we only present some selected samples of each material (hafnium or vanadium nitrides). More complete results for hafnium nitrides will be published in a separate paper. Table 1 summarizes the operating conditions. The film composition was determined by WDS using an electron energy of 4 keV. The apparatus used is a JEOL JSM 5900-LV. The crystal structures of the films, deposited on a Si(100) substrate, were identified by XRD measurements, using a Siemens D-5000 diffractometer with a monochromatic Cu Kα_1 radiation (35 kV, 25 mA) in the symmetric $\theta/2\theta$ geometry. The film thicknesses were determined by XRR with the help of a X'Pert Philips apparatus using also a monochromatic Cu Kα_1 radiation (40 kV, 50 mA). Optical reflectance spectra were recorded within an UV-Vis-IR spectrophotometer (PERKIN-ELMER trade). A commercial barium sulfate ($BaSO_4$) reference was used as blank reference for all reflectance spectra measurements.

3 Results and discussions

3.1 Nitrogen concentration and film thickness

Nitrogen concentration in the obtained films was measured by means of WDS technique. The analyzed zone presents a depth of 100 nm and a diameter of also 100 nm. The peak intensities ratio of nitrogen and vanadium or hafnium of each spectrum allows calculating the nitrogen concentration of the corresponding layer. Table 2 presents the evolution of N/V and N/Hf ratios of the selected films as a function of nitrogen gas flow. Let us make two remarks. The first one is that the increase in nitrogen flow does not induce a proportional increase in nitrogen concentration for both systems: in both cases the variation of flow is important, whereas the stoichiometry practically does not vary. The second one is that in both systems a concentration limit is reached, 1.25 for HfN and 0.83 for VN. The VN system reaches its limit in the substoichiometric region. However, the HfN system remains in the over-stoichiometric region.

Deposited film thicknesses were evaluated by X-ray reflectivity measurements. Let us recall here that Kiessig fringes are the result of interferences between beams

Table 2. Stoichiometry, crystallographic structure and optical parameters for HfN and VN films.

Sample	Stoichiometry (N/Hf atomic ratio)	Crystallographic structure	ω_p' (10^{15} Hz)	$1/\tau$ (10^{15} Hz)	ω_t (10^{15} Hz)	ε_m	ε_d
HfN4	1.19	$\delta-$HfN	4.46*	1.08*	–	30.47*	–
HfN5	1.18	$\delta-$HfN	4.35*	0.97*	–	22.10*	–
HfN6	1.25	$\delta-$HfN	3.77	1.27	3.05	15.87	0.60
HfN7	1.24	$\delta-$HfN	3.28	1.62	1.87	13.79	1.63

Sample	Stoichiometry (N/Hf atomic ratio)	Crystallographic structure	ω_p' (10^{15} Hz)	$1/\tau$ (10^{15} Hz)	ω_t (10^{15} Hz)	ε_m	ε_d
VN6	0.83	$\delta-$VN	3.63	2.65	0.69	0	7.29
VN8	0.82	$\delta-$VN	3.59	2.81	0.69	1.00	6.41
VN10	0.83	$\delta-$VN	3.69	2.91	0.71	2.95	10
VN12	0.78	$\delta-$VN	3.64	2.84	0.51	1.00	6.49

*: Parameters calculated by means of a Drude model. All other values were calculated within an extended Drude model.

reflected at the film surface and beams reflected at the film–substrate interface. They appear in the low-angle reflection domain and allow the determination of thickness with high accuracy, as long as the film thickness remains below approximately 120 nm (which is the case in this study) and the error bar does not exceed the nanometer. Table 1 summarizes thicknesses of the selected films. Let us stress that all samples within the present study were in the nanoscale region. The thickness is less than 70 nm for hafnium nitrides as well as vanadium nitrides.

3.2 Crystallographic structures

Figures 1a–1c show XRD patterns of the considered HfN samples. The examination of XRD spectra makes it possible to affirm that the obtained layers crystallize in NaCl type structure. Although the nitrogen concentrations are higher than 50% (over-stoichiometry), the synthesized samples present only one phase. One can see that the (111) and (200) peaks are narrow and well defined. This confirms a good crystallization of the HfN samples, contrary to the case of V-N systems.

In a previous paper [7], X-ray Diffraction (XRD) measurements of VN samples showed that films deposited at 150 °C, at low nitrogen gas flows (1 and 2 sccm), exhibit an hexagonal sub-nitride phase β-V_2N. From 3 sccm to 15 sccm, the dominant phase in the obtained VN films is a NaCl type phase: δ-VN mononitride [12,13] (see Tab. 1), However, all XRD spectra gave evidence that parts of the considered films are in amorphous forms. Only the (111) peak appears clearly. The XRD patterns in Figures 1d–1f were characterized by an important background as well as intense and broadened peaks which are shifted towards smaller angles.

Let us point out that the principal difference between the two above systems is that VN is partly amorphous whereas HfN is well crystallized. The consequence of this difference, as it will appear clearly later, is that the optical properties are sensitive to stoichiometry and structure.

3.3 Optical properties

The optical reflectance curves, corresponding to the considered various samples are given in Figure 2. All spectra exhibit a deep minimum of reflectance in the visible domain and a maximum in the infrared domain. To determine the optical constants by fitting the reflectance spectra, we used the dielectric function given by the Drude model [15–17] for the metallic cases, equation (2), and the one given by an extended Drude's model, equation (4), for the non-metallic cases. Let us briefly recall the formalism used here to deduce optical constants by fitting the optical reflectance spectra. The normal incidence reflectivity $R(\omega)$ is expressed via the dielectric function $\varepsilon_r(\omega)$ according to the following Fresnel formula [19]:

$$R = \left| \frac{1 - \sqrt{\varepsilon_r(\omega)}}{1 + \sqrt{\varepsilon_r(\omega)}} \right|^2 \tag{1}$$

with respect to frequency ω, the dielectric function $\varepsilon_r(\omega)$ can be cast into several forms [10]. Generally those forms can be determined using the Drude model which describes the free electron contribution to the dielectric function within the framework of a classical point of view [16, 17]. For non-stoichiometric VN and HfN experimental reflectivity spectra, we then used the Drude dielectric function:

$$\varepsilon_r(\omega) = \varepsilon_{hf} \left(1 - \frac{\omega_p'^2}{\omega^2 + i\omega/\tau} \right) \tag{2}$$

$$\omega_p' = \sqrt{\frac{4\pi n e^2}{m^*}}. \tag{3}$$

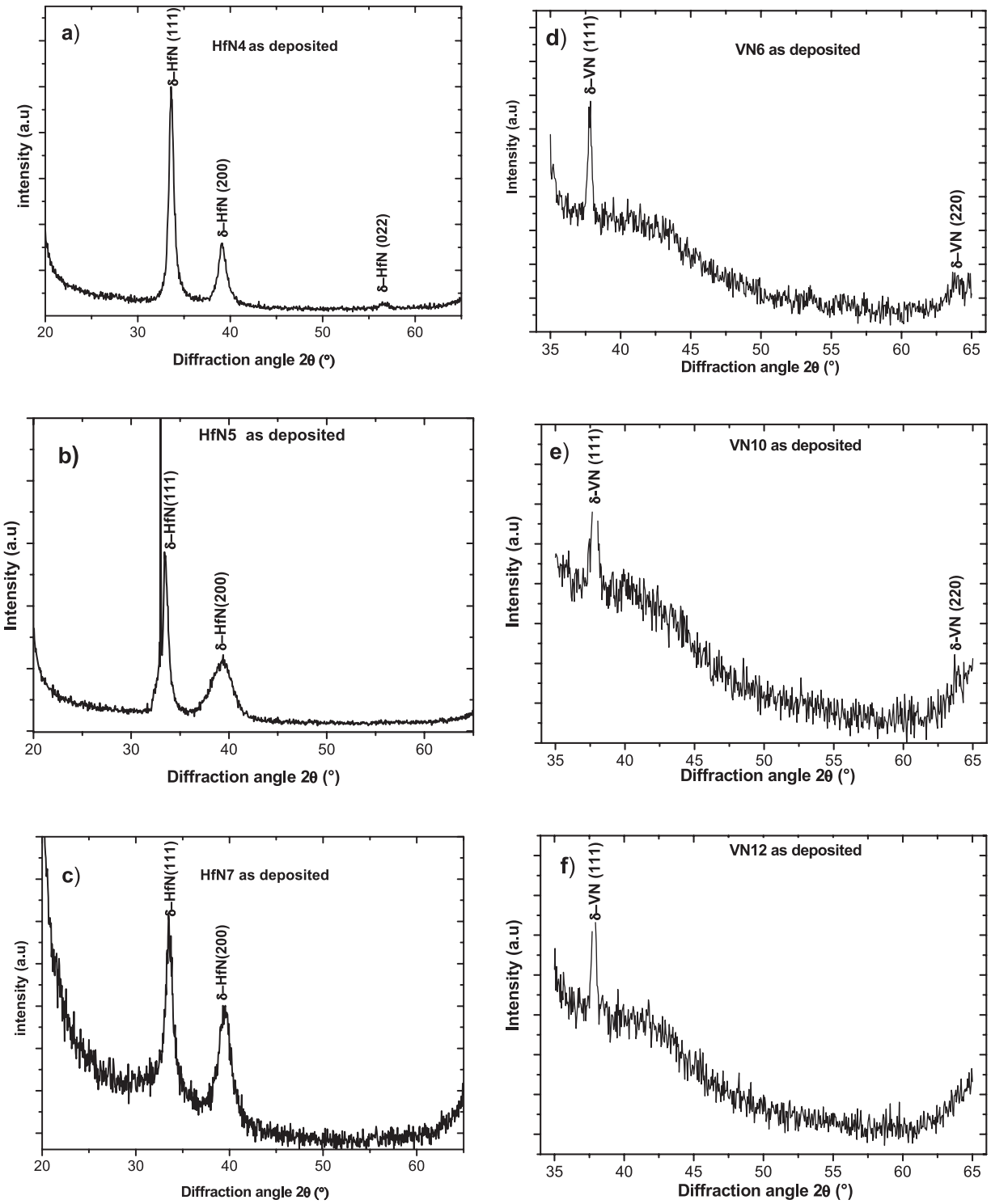

Fig. 1. XRD $\theta - 2\theta$ patterns of (a) HfN4, (b) HfN5, (c) HfN7 and (d) VN6, (e) VN10, (f) VN12 films grown on Si (100) substrate at 150 °C.

In equation (2), ε_{hf} represents the background constant (larger than unity) due to the contribution of higher energy transitions. The Drude term contains a damping factor $1/\tau$ (where τ is the free electron relaxation time) as well as a screened plasma energy ω_p' which is related to the free electron density n, the electron charge e and the effective mass m^* (Eq. (3)). However, for non-metallic samples, we used an extended Drude's model, where the dielectric function becomes [15,18]:

$$\varepsilon_r(\omega) = \varepsilon_m\left(1 - \frac{\omega_p'^2}{\omega^2 + i\omega/\tau}\right) + \varepsilon_d\left(1 - \frac{\omega_p'^2}{\omega^2 - \omega_t^2 + i\omega/\tau}\right). \quad (4)$$

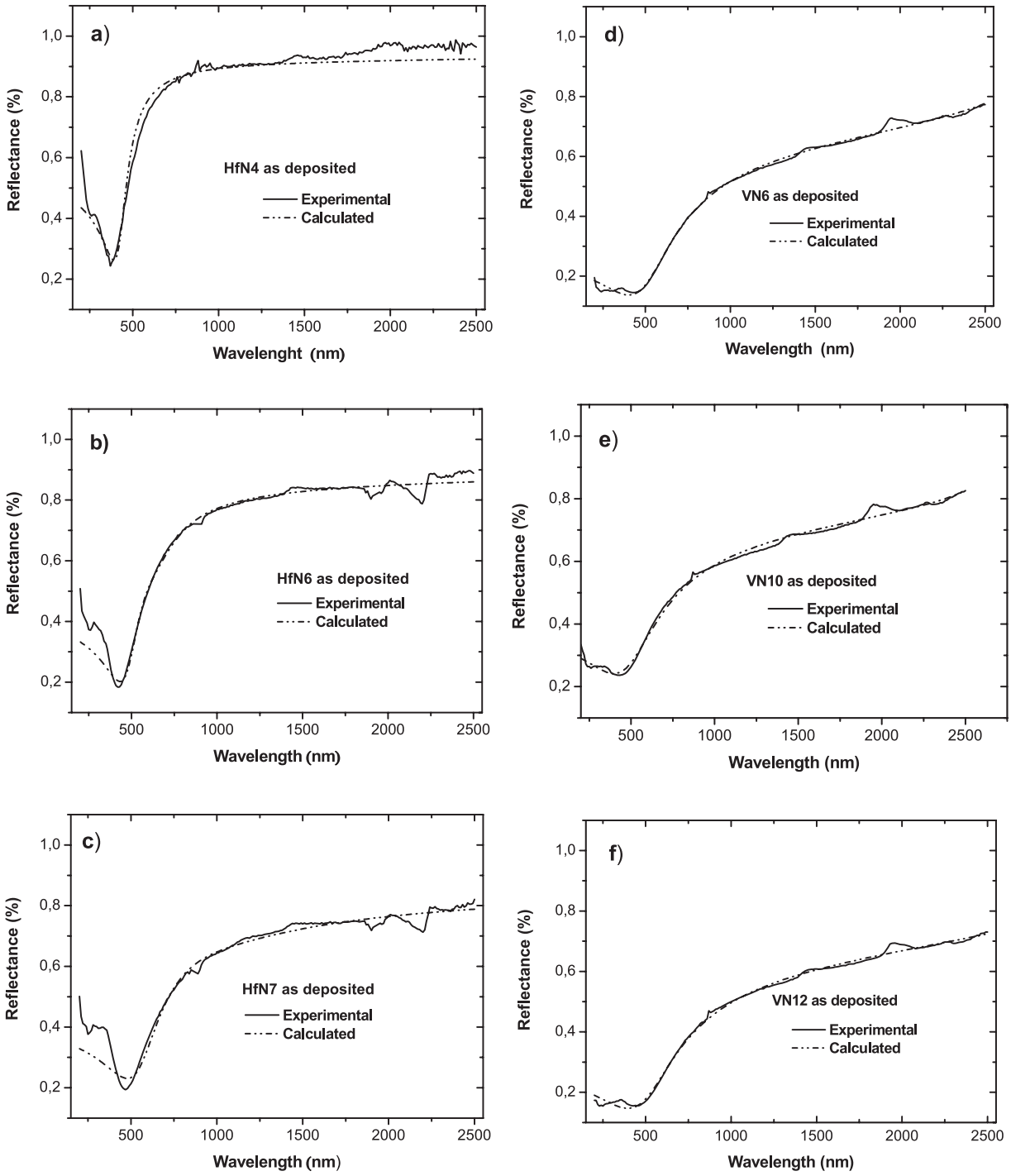

Fig. 2. Experimental (continuous line) and theoretical (dashed line) optical reflectance spectra: (a) HfN4, (b) HfN6, (c) HfN7 and (d) VN6, (e) VN10, (f) VN12.

Equation (4) takes into account the energy gap $E_g = \hbar\omega_t$ between valence and conduction bands ($\hbar$ being the Planck constant over 2π and ω_t a transition frequency). Here the plasmon frequency is expressed by:

$$\omega_p^2 = \left(\omega_p'\right)^2 (\varepsilon_m + \varepsilon_d) \quad (5)$$

where ε_m and ε_d characterize metallic and non-metallic behaviors. The aim of this section is to show the evolution of optical reflectivity, not only versus stoichiometry but also with respect to the film atomic structure. Thus we present here a selection of reflectance spectra for the considered VN and HfN samples (Fig. 2). All corresponding optical spectra expressed a lower reflectivity in the

200–500 nm range. In Figure 2, let us remark that the HfN samples are more reflective than the VN ones in the entire infrared region. Also, according to Figure 2, there is a good agreement between experimental and calculated spectra. All results were reported in Table 2. In the case of vanadium nitride films, we can point out that the ε_m constant values tend towards zero. Consequently, the metallic contribution is less important than the non-metallic one. Since Figure 2 shows both experimental and calculated optical reflectance spectra in a consistent way, we can conclude that the dielectric Drude function, applied to transition metal nitrides, allows having good agreement in fitting experimental spectral reflectivity.

Furthermore, the dielectric contribution becomes rather significant. Except for HfN4 and HfN5 samples, we obtain a good theoretical fit with the help of an extended Drude dielectric function for all other samples. We should also mention that in the case of VN films we attempt to fit with a unique Drude dielectric function but we did not succeed. One reason for that is the existence of an amorphous part in the VN films. Also, let us notice that in the considered samples the screened plasma frequency ω_p' varies very little versus nitrogen flow (practically constant for VN case; see Tab. 2). Using Drude and extended Drude models for various optical reflectivity spectra, we were successfully able to adjust calculated results to experimental ones. This procedure enabled us to determine optical constants (Tab. 2) such as refraction index n and extinction coefficient k. The refraction index n and extinction coefficient k have been calculated following their usual definition:

$$n + \mathrm{i}k = \sqrt{\varepsilon_r}. \tag{6}$$

The dielectric function ε_r is written in the following form:

$$\varepsilon_r(\omega) = \varepsilon_1(\omega) + \varepsilon_2(\omega). \tag{7}$$

From equations (6) and (7), the optical constants n and k can be written as follows:

$$n = \frac{1}{\sqrt{2}} \left[\sqrt{\varepsilon_1^2 + \varepsilon_2^2} + \varepsilon_1 \right]^{\frac{1}{2}} \tag{8}$$

$$k = \frac{1}{\sqrt{2}} \left[\sqrt{\varepsilon_1^2 + \varepsilon_2^2} - \varepsilon_1 \right]^{\frac{1}{2}}. \tag{9}$$

The layouts of refraction index n and extinction coefficient k of HfN and VN with respect to irradiation wavelength, show (Fig. 3) a non-metal behavior at high wavelength ($n > 1$). The basic reason for transparent heat mirror properties of a single thin film is the combination of a low n value in the visible part of the spectrum and an increased k value near the infrared region. This behavior is typical for a free-electron-like situation as originally described by Drude's model. In Figure 3, the extinction coefficient k explicitly showed the same evolution.

Stromme et al. [19] reported that the optical constants change with thickness in HfN systems. This effect was not observed in our study because all samples have the same thickness. In Figures 3a–3c, we can see that the k constant varies little in the visible region. Moreover the optical constants decrease quickly in the infrared region when the nitrogen flow increases. We think that the increase in defects concentration in HfN films and the reduction in grains size, which reduce the electrons mean free path, is at the origin of this behaviour [8]. We notice, however, a completely differing behaviour for VN films Figures 3d–3f, where the optical constant is less sensitive to the variations of flow. For VN systems, the relaxation time constant varies very little with nitrogen flow (Tab. 2). It should be pointed out that, practically, the various VN samples do present the same nitrogen concentration as well as crystallographic structure. This could explain why Figures 3d–3f are very similar.

4 Conclusion

Vanadium and hafnium nitride nanoscale films were synthesized onto (100)-oriented silicon wafers by reactive dc-magnetron sputtering. The temperature of the substrate was fixed at 150 °C. The experimental conditions are selected in order to achieve two goals. The first one was to obtain ultra thin layers (in the nanoscale range). The second one was to be able to compare two symmetric systems: over-stoichiometric hafnium nitrides and sub-stoichiometric vanadium nitrides. This was carried out experimentally with full success. The XRR results revealed that all synthesized films have approximately the same thickness in the nanoscale range (less than 70 nm). The measured nitrogen concentration, by means of WDS, induced sub-stoichiometric samples for vanadium nitrides and over-stoichiometric samples for hafnium nitrides. XRD patterns showed that the crystallographic film structure is of NaCl type for both systems. The optical constants of the obtained films were derived from the reflectance spectra by means of the extended Drude model. Good agreement was found between experimental and calculated optical reflectance. Only HfN4 and HfN5 films exhibited a pronounced metallic behavior. The VN samples presented a large non-metallic behavior. This was explained by the presence of an amorphous phase. The HfN samples are characterized by a better optical behaviour than the VN samples.

The authors would like to thank both referees for their careful reviewing and pertinent remarks.

References

1. M.Y. Liao, Y. Gotoh, H. Tsuji, J. Ishikawa, J. Vac. Sci. Technol. A **22**, 146 (2004)
2. H.M. Benia, M. Guemmaz, G. Schmerber, A. Mosser, J.C. Parlebas, J. Appl. Surf. Sci. **200**, 231 (2002)

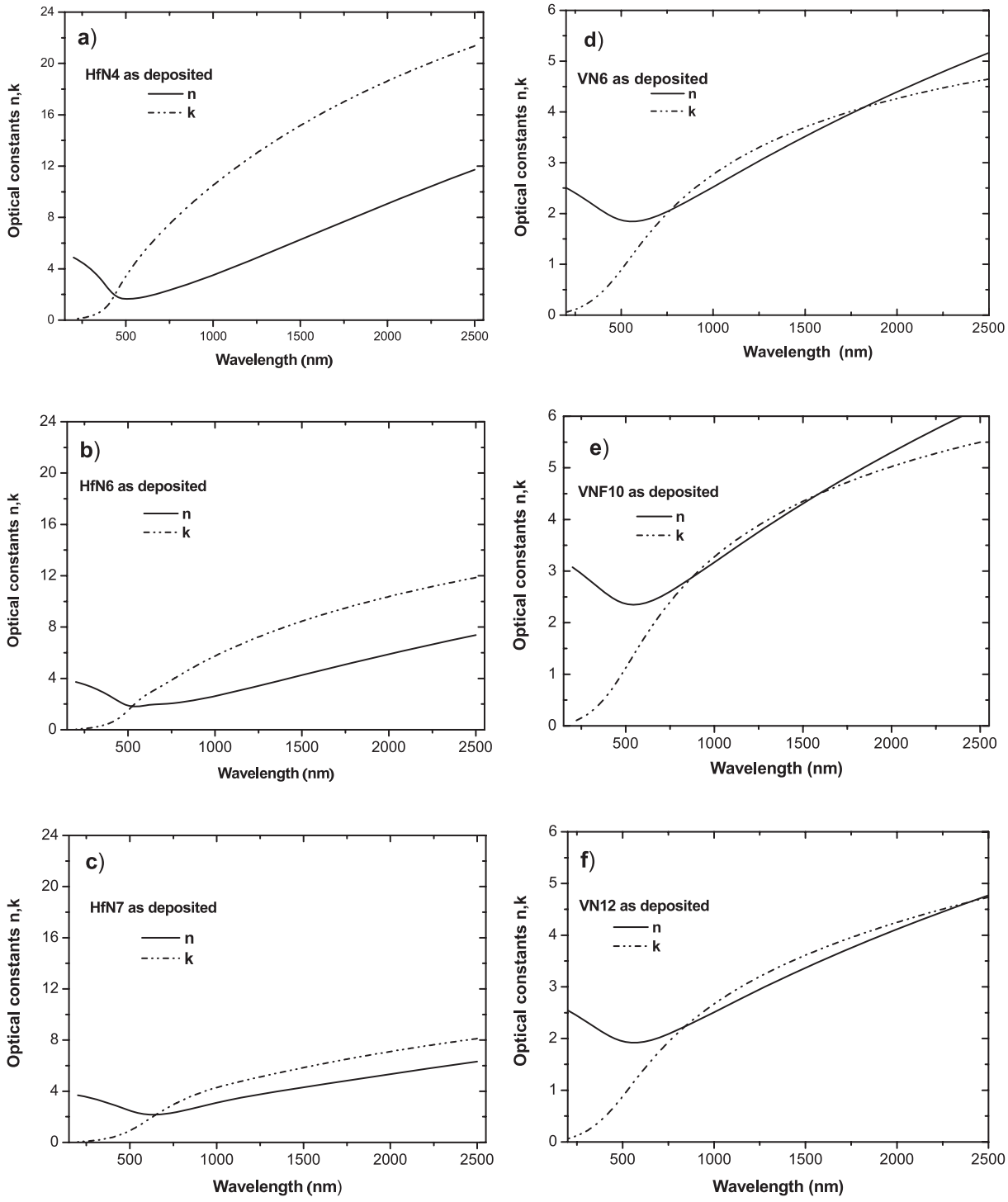

Fig. 3. Optical constants (refraction index n and extinction coefficient k) derived by fitting experimental spectra with the Drude model and extended Drude model: (a) HfN4, (b) HfN6, (c) HfN7 and (d) VN6, (e) VN10, (f) VN12.

3. M. Torche, G. Schmerber, M. Guemmaz, A. Mosser, J.C. Parlebas, Thin Solid Films **436**, 208 (2003)
4. L. Pichon, T. Girardeau, A. Straboni, F. Lignou, P. Guerra, J. Perriere, J. Appl. Surf. Sci. **150**, 115 (1999)
5. K.L. Ou, M.H. Tsai, H.M. Huang, S.Y. Chiou, C.T. Lin, S.Y. Lee, Microelec. Eng. **77**, 184 (2005)
6. K.L. Ou, Microelec. Eng. **83**, 312 (2006)
7. H. Gueddaoui, G. Schmerber, M. Abes, M. Guemmaz, J.C. Parlebas, Cat. Today **113**, 270 (2006)
8. S. Maabed, *Magister Thesis*, Faculty of Sciences (University of Setif, 2007)
9. M. Stromme, R. Karmhag, C.G. Ribbing, Opt. Mat. **4**, 629 (1995)

10. T. Easwarakhanthan, M.B. Assouar, P. Pigeat, P. Alnot, J. App. Phys. **98**, 73531 (2005)
11. W.M. Gnehr, U. Hartung, T. Kopte, Thin Solid Films **478**, 142 (2005)
12. T.B. Massalski, *Binary Alloy Phase Diagram*, AMS (Metals Park, OH, 1991)
13. E. D'Anna, A. Di Cristoforo, M. Fernandez, G. Leggieri, A. Luches, G. Majni, L. Nanai, Appl. A. Delin, O. Eriksson, R. Ahuja, B. Johansson, M.S.S. Brooks, T. Gasche, Surf. Sci. **186**, 496 (2002)
14. P. Kroll, Phys. Rev. Lett. **90**, 125501 (2003)
15. J. Casaux, *Physique du solide* (Masson, Paris, 1981)
16. P. Drude, Ann. Phys. (Leipzig) **1**, 566 (1900)
17. P. Drude, Ann. Phys. (Leipzig) **3**, 369 (1900)
18. H.M. Benia, M. Guemmaz, G. Schmerber, A. Mosser, J.C. Parlebas, Cat. Today **89**, 307 (2002)
19. M. Stromme, R. Karmhag, C.G. Ribbing, Opt. Mat. **4**, 629 (1995)